Effect of inlet conditions in hydrogen–air supersonic reactive mixing layers

César Huete[1], Pedro J. Martinez-Ferrer[2,4], Daniel Martínez-Ruiz[3], Daniel Mira[4]

[1] Universidad Carlos III de Madrid, Leganés, Madrid, Spain
[2]Universitat Politécnica de Catalunya, Barcelona, Spain
[3]Universidad Politécnica de Madrid, Madrid, Spain
[4]Barcelona Supercomputing Center, Barcelona, Spain

1 Introduction

The chemical reaction of two supersonic flow streams of fuel and oxidizer is of great interest to the development of advanced hypersonic systems for aircraft propulsion such as scramjets. A large number of numerical studies have provided fundamental insights and valuable explanations to the dynamics and flow structure of supersonic mixing layers [1–3] and to their reactive extension [4–6]. It is well known that the inlet condition can have strong influence on the growth rate of the mixing layer, the formation of coherent structures and the roll-up characteristics [7]. However, to the best of the authors knowledge, little debate has been presented on the virtual origin of canonical compressible mixing layers. In particular, Sandham and Reynolds [8] explored some of the numerical modifications of the inlet plane in incompressible mixing layers by comparing typical hyperbolic tangent and wake-type modified velocity profiles. Ko et al. [9] explored the effect of perturbing the inflow of the incompressible mixing layer. On the other hand, the vast majority of numerical studies have focused on the temporal evolution of shear and mixing layers due to computational costs and because they provide a satisfactory approximation of the laboratory spatially-developing mixing layers; however, this correlation is only valid when the slip velocity between the two streams is smaller than the convective velocity [10]. For high-speed flows such as the ones addressed herein, this assumption is inaccurate and needs to be revisited.

In particular, the numerical study of supersonic coflows demands the choice of appropriate inlet conditions that describe the inner structure of the mixing layer. Typically, this is carried out by assuming a smooth hyperbolic function in the form: $U(y) \sim \tanh^{-1}(y/\delta)$, where y is the transverse coordinate, δ is a characteristic mixing layer thickness (typically, the initial vorticity thickness $\delta_{\omega,0}$), and U is the streamwise velocity function [8, 11]. This formulation suffices to describe most of the canonical shear layers. Mixing layers, on the other hand, demand the definition of inner profiles for each of the species in the mixture $Y_i(y)$, with the values determined by far-field conditions: $[U_1, Y_{i,1}]$ for the upper stream and $[U_2, Y_{i,2}]$ for the lower one. In addition, temperature has a major relevance as it affects the density and, therefore, the inertia of the flow. Moreover, temperature is also involved in the definition of the upper and lower stream Mach numbers, $M_1 = U_1/c_1$ and $M_2 = U_2/c_2$, respectively, with $c = \sqrt{\gamma p/\rho} = \sqrt{\gamma R_g T}$ standing for the sound speed, $\gamma = c_p/c_v$ and R_g being the ratio of specific heats and the gas constant, respectively, and p and ρ referring to pressure mixture and density. The latter is directly related to the mass fraction of the species involved through $Y_i = \rho_i/\rho$. Therefore, as long as thermal diffusion is of the same order as species diffusion in gases, that is Lewis number $\mathrm{Le} \sim \mathrm{O}(1)$, temperature profiles are key to describe the mixing layer developing thickness.

Correspondence to: chuete@ing.uc3m.es

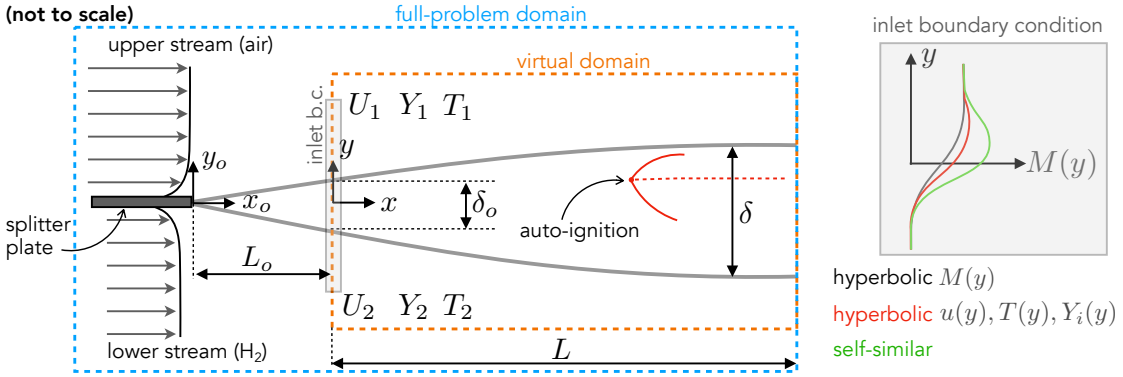

Figure 1: Sketch of the laminar mixing layer domains and the arbitrary choice of the inlet conditions in the virtual computational domain.

The effect of imposing different inner profiles of the state variables on the ignition distance of a supersonic mixing layer problem is explored here. In particular, the problem of a supersonic hydrogen–air mixing layer, similar to the experiment conducted by Cheng et al. [12], is investigated using direct numerical simulations. A sketch of the setup with the computational domain used for numerical simulations and the arbitrary choice of the inlet conditions is shown in Fig. 1. It can be seen that boundary conditions for U, Y_i, and T for each stream must be provided to define a well-posed mathematical problem. The choice of the inlet condition may have a potential impact in the prediction of the autoignition distance, particularly in high-speed reactive mixing layers where a variation of the order of milliseconds in the autoignition time, owing to a miss-calculation of the mixing layer state, is translated into distances of the order of meters, the characteristic length of a supersonic combustion chamber. In the following, the ideal gas law is assumed for both streams and, since the mixture is mostly made of diatomic gases at conditions of interest, the adiabatic index is taken constant, $\gamma_1 = \gamma_2 = \gamma = 7/5$. Besides, pressure is assumed to be uniform at the inlet, so the following relationships apply to molecular weights, $W_1\rho_2T_2 = W_2\rho_1T_1$, and Mach numbers, $M_1U_2\sqrt{\rho_1} = M_2U_1\sqrt{\rho_1}$ outside of the mixing layer.

1.1 Hyperbolic functions for the inlet variables

The arbitrariness in the inlet condition relies in the choice of the inner profiles for the mixing layer. For example, Fig. 1 depicts the laminar mixing layer domains and the arbitrary choice of the inlet conditions in the computational domain. Beforehand, we could make use of the hyperbolic inlet condition for either of the independent variables, namely

$$\phi(\bar{y}) = \frac{\phi_1 + \phi_2}{2} + \frac{\phi_1 - \phi_2}{2}\tanh^{-1}(\bar{y}), \tag{1}$$

where $\bar{y} = y/\delta$ is the scaled order-of-unity transverse coordinate and ϕ represents any suitable inlet conditions for the streamwise velocity (transverse velocity is set to a zero value), temperature, and $N-1$ species mass fractions. On condition that pressure is uniform and known, $\sum_1^N Y_i = 1$ and the equation of state are used to compute the N^{th} species and the density field. In our case, the mixture composition in the upper and lower streams is given by $Y_{H_2,1} = 0$, $Y_{O_2,1} = 0.233$, and $Y_{N_2,1} = 0.767$, and $Y_{H_2,2} = 1$ and $Y_{O_2,2} = Y_{N_2,2} = 0$, respectively. By choosing also the velocity and the temperature of the outer streams $[U_1, T_1]$ and $[U_2, T_2]$, the rest of the flow variables can be derived, as stated above. A widely-used approach to prescribe these quantities is the Buseman–Crocco velocity–temperature relation [3, 5], a very particular choice far from validity in general applications.

Alternatively, the Mach number profile could be imposed to follow the hyperbolic relation given by Eq. (1) so that U must be transformed into a dependent variable. This inlet condition for $M(\bar{y})$ is appealing as it directly provides the convective Mach number $M_c = M_1 - M_2$ as an input parameter, which is known to play a dominant role in the description of the laminar–turbulent flow transition in high-speed conditions. Nevertheless, for hydrogen–air mixing layers, the stream containing hydrogen is much lighter than the oxidizer stream, and thermodiffusive effects can play an important role on the composition and thermal field along the mixing layer development. In fact, none of the above-prescribed hyperbolic inlet conditions occurs as the natural solution of a truly evolving mixing layer.

1.2 Self-similar mixing layer for the inlet variables

A more appropriate definition of the inlet condition is based on the assumption that the flow evolves laminarly from the leading edge of the thin splitter plate. Here, the relevant Reynolds number of the flow $Re = \rho_1 U_1 L_o/\mu_1$, is based on the velocity U_1, density ρ_1, and shear viscosity μ_1 of the upper stream. It results in a slender mixing layer, whose characteristic thickness increases according to $[(\mu_1/\rho_1)x_o/U_1]^{1/2}$, reaching a value of $\delta_o \sim O(\mathrm{Re}^{-1/2}L_o) \ll L_o$ at $x_o = L_o$. Since nitrogen and oxygen have similar molecular weights, the ratio of the species along the mixing layer can be assumed to be constant until the autoignition point. Consequently, it can be assumed that the mixing process is equivalent to that of a binary mixture between fuel and air. Therefore, the corresponding fuel diffusion flux, non-dimensionalized by $[\rho_1\mu_1 U_1/L_o]^{1/2}$, can be computed with an explicit form [13,14], as given by the second equality in (5). It accounts for mass and thermal diffusion, the latter having a significant effect for hydrogen. Here, $\bar{T} = T/T_1$ and $\bar{\rho} = \rho/\rho_1$ correspond to the dimensionless temperature and density functions, respectively, and $\eta = y/[(\mu_1/\rho_1)x/U_1]^{1/2}$ represents the order-of-unity self-similar variable. The Prandtl number $Pr = \mu c_p/\lambda = 0.7$ throughout the non-reactive zone, with λ and c_p representing the thermal conductivity and the specific heat at constant pressure of the mixture, respectively. The ratio of the thermal diffusivity $\lambda/(\rho c_p)$ to the fuel–air binary diffusion coefficient D is the so-called Lewis number $Le = \lambda_1/(\rho_1 c_{p1} D_1)$ that includes the dimensionless binary diffusion coefficient $\bar{D} = D/D_1$. The thermal diffusion factor α, defined as the ratio of the thermal diffusion coefficient to the product $Y(1-Y)\rho D$, is taken constant, with $\alpha \approx -0.3$ for hydrogen–air mixtures [14].

Considering the scaling of the quantities with the above dimensionless variables, the conservation equations for the boundary value problem used to define the inlet conditions can be written as:

$$-\frac{\eta}{2}\frac{\mathrm{d}}{\mathrm{d}\eta}\left(\bar{\rho}\bar{u}\right) + \frac{\mathrm{d}}{\mathrm{d}\eta}\left(\bar{\rho}\bar{v}\right) = 0\,, \tag{2}$$

$$\bar{\rho}\left(\bar{v} - \frac{\eta}{2}\bar{u}\right)\frac{\mathrm{d}\bar{u}}{\mathrm{d}\eta} = \frac{\mathrm{d}}{\mathrm{d}\eta}\left(\bar{\mu}\frac{\mathrm{d}\bar{u}}{\mathrm{d}\eta}\right)\,, \tag{3}$$

$$\begin{aligned}\bar{\rho}\bar{c}_p\left(\bar{v} - \frac{\eta}{2}\bar{u}\right)\frac{\mathrm{d}\bar{T}}{\mathrm{d}\eta} &= \frac{1}{Pr}\frac{\mathrm{d}}{\mathrm{d}\eta}\left(\bar{\mu}\bar{c}_p\frac{\mathrm{d}\bar{T}}{\mathrm{d}\eta}\right) - (\bar{w}_2^{-1} - 1)\bar{j}\frac{\mathrm{d}\bar{T}}{\mathrm{d}\eta} - \frac{\alpha(\gamma-1)}{\bar{w}_2\gamma}\frac{\mathrm{d}}{\mathrm{d}\eta}\left(\bar{w}\bar{j}\bar{T}\right)\\ &\quad + (\gamma-1)M_1^2\bar{\mu}\left(\frac{\mathrm{d}\bar{u}}{\mathrm{d}\eta}\right)^2\,,\end{aligned} \tag{4}$$

$$\bar{\rho}\left(\bar{v} - \frac{\eta}{2}\bar{u}\right)\frac{\mathrm{d}Y}{\mathrm{d}\eta} = -\frac{\mathrm{d}\bar{j}}{\mathrm{d}\eta} = \frac{1}{PrLe}\frac{\mathrm{d}}{\mathrm{d}\eta}\left[\bar{\rho}\bar{D}\left(\frac{\mathrm{d}Y}{\mathrm{d}\eta} + \alpha\frac{Y(1-Y)}{\bar{T}}\frac{\mathrm{d}\bar{T}}{\mathrm{d}\eta}\right)\right]\,, \tag{5}$$

where $\bar{u} = u/U_1$, $\bar{v} = v/U_1(L_o/\delta_o)$, $\bar{\mu} = \mu/\mu_1$, $\bar{c}_p = c_p/c_{p1}$ and $\bar{w} = W/W_1$ are the shear viscosity, specific heat, and mean molecular weight scaled with their air stream values. The above equations must

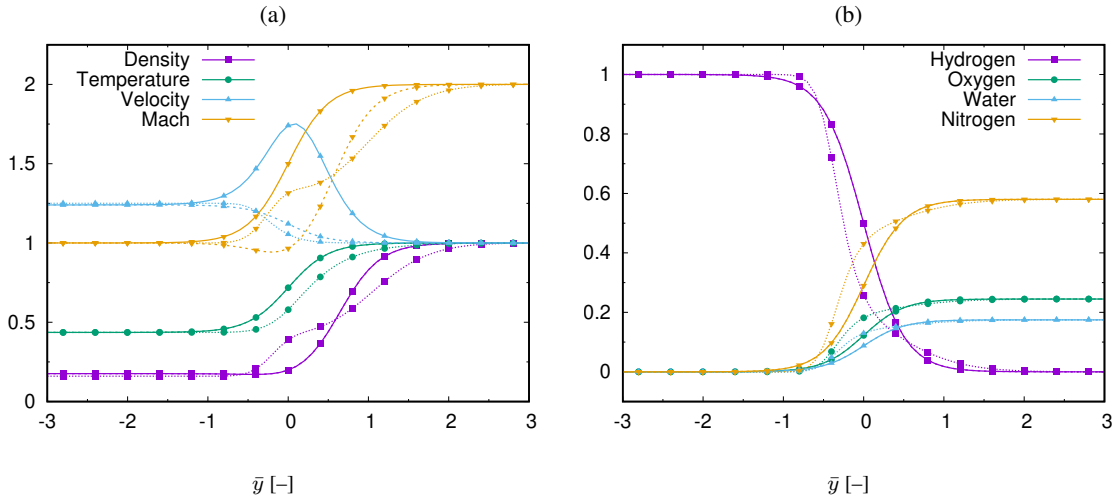

Figure 2: (a) Nondimensional flow variables and (b) mass fraction inlet profiles across the nondimensional transverse coordinate: hyperbolic Mach number (solid line), hyperbolic streamwise velocity (dashed line), and self-similar solution (dotted line). Reference values are $\delta_{\omega,0} = 1.78 \times 10^{-3}\,\mathrm{m}$, $\rho_{\mathrm{ref}} = 0.278\,\mathrm{kg/m^3}$, $T_{\mathrm{ref}} = 1250\,\mathrm{K}$, and $U_{\mathrm{ref}} = 1429\,\mathrm{m/s}$.

be supplemented with the equation of state $\bar{\rho}\bar{T} = \bar{w} = \left[1 + (\bar{w}_2^{-1} - 1)Y\right]^{-1}$, and with the expressions

$$\bar{\mu} = \frac{1 + [\bar{\mu}_2/\bar{w}_2^{1/2} - 1]Y}{1 + (\bar{w}_2^{-1/2} - 1)Y}\bar{T}^{\sigma_1}\ ,\ \bar{D} = \bar{T}^{1+\sigma_1}\ ,\ \text{and}\ \bar{c}_p = [1 + (\bar{w}_2^{-1} - 1)Y]\bar{T}^{\sigma_2}\ , \tag{6}$$

to account for the variation of the transport coefficients and specific heat with temperature and composition. The representative values $\sigma_1 = 0.7$ and $\sigma_2 = 0.2$ are used for the temperature power laws [15]. An example of how different inlet conditions affect the mixing-layer profile, with the conditions of the experiment of Cheng et al. [12], is shown in Fig. 2. When imposing the velocity profile, the Mach number is not a monotonic function and attains subsonic conditions at an intermediate position. This effect is of pivotal importance because downstream pressure disturbances can reach the inlet plane through the subsonic region. In addition, if an oblique shock is considered to promote the ignition (as occurs in scramjet engines), the penetration length into the mixing layer would be shortened and the post-shock flow correspondingly affected. Further differences are expected to occur for higher Mach numbers, where the heating associated with viscous dissipation, see last term in (4), could be sufficiently intense to promote the appearance of a local maximum inside the mixing layer [16], thereby placing the ignition kernel far inside from the hot upper stream.

2 Direct Numerical Simulations

Direct numerical simulations (DNS) for the evolution of the reactive mixing layer with different inlet boundary conditions are offered in Fig. 3. It is shown three instantaneous temperature fields associated with the three conditions employed in Fig. 2, which share the same flow properties outside the mixing layer. The numerical simulations have been carried out with CREAMS [17], a compressible reactive Navier–Stokes solver that uses a spatial seventh-order WENO scheme and a third-order total variation diminishing Runge–Kutta temporal scheme. The value of the initial vorticity thickness, $\delta_{\omega,0} = 1.78 \times 10^{-3}\,\mathrm{m}$, is calculated from the inlet Reynolds number $\mathrm{Re}_{\omega,0} = 3200$ and the average and convective flow properties are provided from experimental data [12]. By direct inspection of Fig. 3, it is evident that,

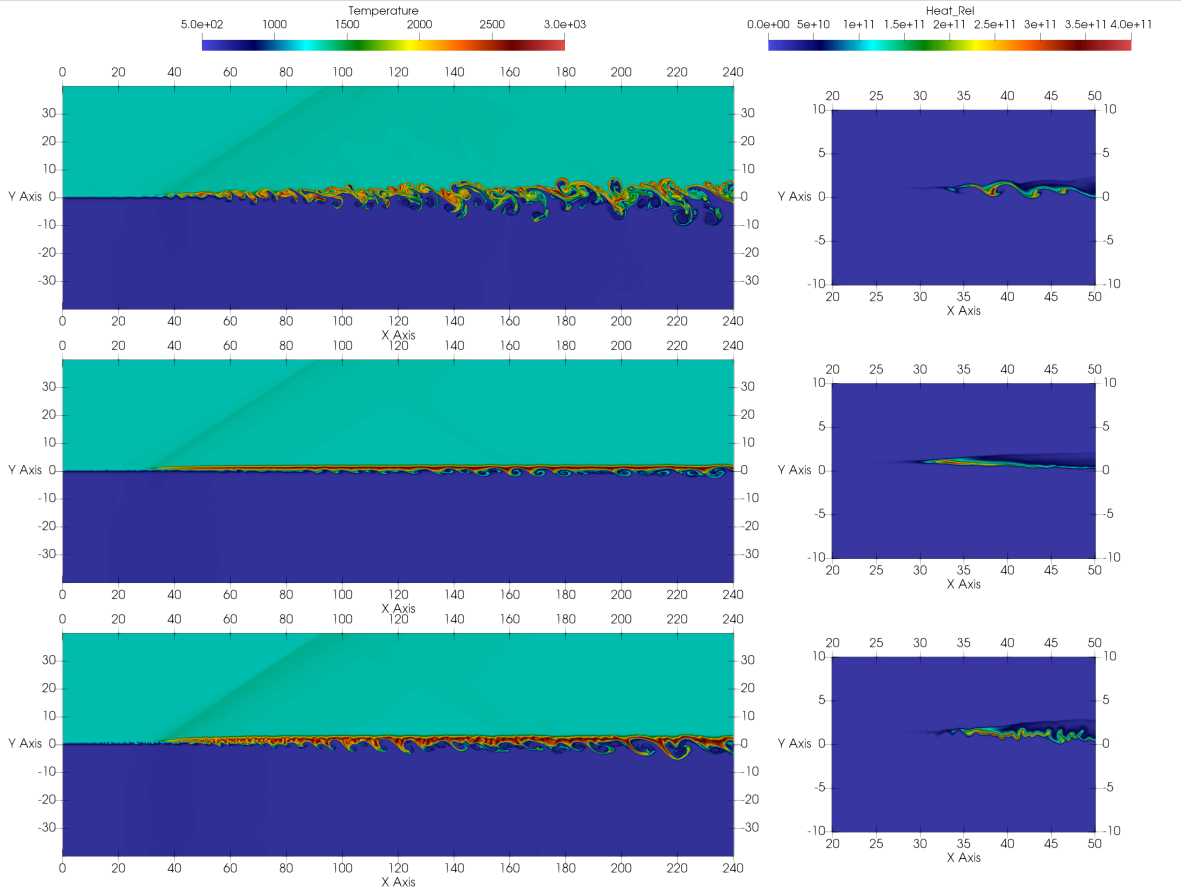

Figure 3: Instantaneous temperature and hear release fields corresponding to three initial profiles: hyperbolic Mach number (top), hyperbolic streamwise velocity (middle), and self-similar solution (bottom). Dimensionless spatial coordinates scale with $\delta_{\omega,0} = 1.78 \times 10^{-3}$ m.

under the specified conditions, the turbulent structures vary greatly based on the mixing layer profile. However, the self-ignition distance, measured at the point of maximum reaction rate, is roughly located at a distance of 3 mm from the inlet conditions and remains practically unchanged. The main causes for this outcome are attributed to three factors: (1) the temperature profile does not exhibit significant variations based on the selection of inlet conditions, (2) the air stream is very hot and dominates the thermal runway, and (3) ignition occurs prior to the formation of turbulent structures. This outcome should be analyzed further by considering higher Mach numbers and larger convective Mach numbers, where temperature within the mixing layer may display greater sensitivity to the inlet conditions.

Acknowledgements

The authors gratefully acknowledge Dr. Arnaud Mura, CNRS researcher at Institut PPRIME in France, for the numerical tool CREAMS as well as Dr. Alexandre Ern and Dr. Vincent Giovangigli for the EGLIB software. C.H.and D.M.R work has been funded with projects TED2021-129446B-C41 and TED2021-129446B-C43 funded by MCIN/AEI /10.13039/501100011033 and European Union NextGenerationEU/ PRTR. C.H. and D.M.R. work has been also supported by the Madrid Government (Comunidad de Madrid-Spain) under the Multiannual Agreement with UC3M (H2SFE-CM-UC3M) and UPM (CHAC-CM-UPM). Also the projects MCIN/AEI/10.13039/501100011033 and ESF/10.13039/501100004895 and the Grant RYC2019-027592-I for P.J.M.

References

[1] Sandham, ND. (1989) A numerical investigation of the compressible mixing layer. PhD dissertation. Stanford University.

[2] Leep, LJ, Dutton, JC, and Burr, RF. (1993) Three-dimensional simulations of compressible mixing layers: Visualizations and statistical analysis. AIAA Journal, **31** (11), 2039–2046.

[3] Kourta, A, and Sauvage, R. (2002) Computation of supersonic mixing layers. Physics of Fluids, **14** (11), 3790–3797.

[4] Drummond, JP. (1988) A two-dimensional numerical simulation of a supersonic, chemically reacting mixing layer. NASA STI, 4055.

[5] Menon, S, and Fernando, E. (1990) A numerical study of mixing and chemical heat release in supersonic mixing layers. 28^{th} Aerospace Sciences Meeting, pp-152.

[6] Nishioka, M, and Law, CK. (1997) A numerical study of ignition in the supersonic hydrogen/air laminar mixing layer. Combustion and Flame, **108**, 199–219.

[7] Pirozzoli, S, Bernardini, M., Marié, S, and Grasso, F. (2015) Early evolution of the compressible mixing layer issued from two turbulent streams. Journal of Fluid Mechanics, **777**, 196–218.

[8] Sandham, ND and Reynolds, WC. (1989) Some inlet-plane effects on the numerically simulated spatially-developing mixing layer. Turbulent Shear Flows, **6**, 441–454.

[9] Ko, J, Lucor, D and Sagaut, P. (2008) Sensitivity of two-dimensional spatially developing mixing layers with respect to uncertain inflow conditions. Physics of Fluids, **20** (7), 077102.

[10] Riley, JJ and Metcalfe, RW. (1980) Direct numerical simulation of a perturbed, turbulent mixing layer, AIAA Paper, 1980–274.

[11] Sekar, B, and Mukunda, HS. (1990) A computational study of direct simulation of high speed mixing layers without and with chemical heat release. 23^{rd} Symposium on Combustion, 707–713.

[12] Cheng, TS, Wehrmeyer, JA, and Pitz, RW. (1994) Raman measurement of mixing and finite-rate chemistry in a supersonic hydrogen–air diffusion flame. Combustion and Flame, **99**, 157–173 .

[13] Huete, C, Urzay, J, Sánchez, AL, and Williams, FA. (2016) Weak-shock interactions with transonic laminar mixing layers of fuels for high-speed propulsion. AIAA Journal, **54**(3), 966-979.

[14] Sánchez, AL, and Williams, FA. (2014) Recent advances in understanding of flammability characteristics of hydrogen. Progress in Energy and Combustion Science, **41**, 1–55.

[15] Rosner, DE. (2012) Transport processes in chemically reacting flow systems. Courier Corporation.

[16] Huete, C, Sánchez, AL, Williams, FA, and Urzay, J. (2015) Diffusion-flame ignition by shock-wave impingement on a supersonic mixing layer. Journal of Fluid Mechanics, **784**, 74–108.

[17] Ferrer, PJM, Buttay, RM, Lehnasch, G, and Mura A. (2014) A detailed verification procedure for compressible reactive multicomponent Navier-Stokes solvers. Computers & Fluids, **89**, 88–110.